MOLECULAR AND CELLULAR BIOLOGY, July 2009, p. 3975–3990 Vol. 29, No. 14
0270-7306/09/$08.00+0 doi:10.1128/MCB.01867-08

The Nek6 and Nek7 Protein Kinases Are Required for Robust Mitotic Spindle Formation and Cytokinesis▽§

Laura O'Regan and Andrew M. Fry*

Department of Biochemistry, University of Leicester, Lancaster Road, Leicester LE1 9HN, United Kingdom

Received 8 December 2008/Returned for modification 28 January 2009/Accepted 27 April 2009

Nek6 and Nek7 are members of the NIMA-related serine/threonine kinase family. Previous work showed that they contribute to mitotic progression downstream of another NIMA-related kinase, Nek9, although the roles of these different kinases remain to be defined. Here, we carried out a comprehensive analysis of the regulation and function of Nek6 and Nek7 in human cells. By generating specific antibodies, we show that both Nek6 and Nek7 are activated in mitosis and that interfering with their activity by either depletion or expression of reduced-activity mutants leads to mitotic arrest and apoptosis. Interestingly, while completely inactive mutants and small interfering RNA-mediated depletion delay cells at metaphase with fragile mitotic spindles, hypomorphic mutants or RNA interference treatment combined with a spindle assembly checkpoint inhibitor delays cells at cytokinesis. Importantly, depletion of either Nek6 or Nek7 leads to defective mitotic progression, indicating that although highly similar, they are not redundant. Indeed, while both kinases localize to spindle poles, only Nek6 obviously localizes to spindle microtubules in metaphase and anaphase and to the midbody during cytokinesis. Together, these data lead us to propose that Nek6 and Nek7 play independent roles not only in robust mitotic spindle formation but also potentially in cytokinesis.

When cells divide, they must accurately segregate the duplicated genetic material between two daughter cells such that each receives a single complete set of chromosomes. This complex biomechanical feat is achieved through the action of a bipolar microtubule-based scaffold called the mitotic spindle (36). Microtubules are primarily nucleated by centrosomes that sit at the spindle poles (37). However, microtubule nucleation also occurs in the vicinity of the chromosomes and within the spindle itself (12, 13). These activities combine to ensure the efficient capture of sister chromatids as well as the maintenance of a robust structure capable of resisting the considerable forces required for chromosome separation.

Spindle assembly is regulated in large part by reversible phosphorylation, and a number of protein kinases are activated during mitosis, localize to specific regions of the spindle, and phosphorylate spindle-associated proteins. These include the master mitotic regulator Cdk1/cyclin B, the polo-like kinase Plk1, and the Aurora family kinases Aurora A and B (25). More recently, members of the NIMA-related kinase family have also been implicated in mitotic spindle regulation (27, 29). NIMA was first identified in *Aspergillus nidulans* as a kinase required for mitotic entry, possibly through triggering the relocation of Cdk1/cyclin B to the nucleus (6, 38). NIMA can also phosphorylate S10 of histone H3 to promote chromatin condensation (7). The fission yeast NIMA-related kinase Fin1 contributes to multiple steps in mitotic progression, including the timing of mitotic entry, spindle formation, and mitotic exit (14, 15). However, the detailed mechanisms by which these fungal kinases contribute to mitotic regulation remain far from understood.

In mammals, there are 11 NIMA-related kinases, named Nek1 to Nek11, and of these, 4 have been directly implicated in mitotic regulation, as follows: Nek2, Nek6, Nek7, and Nek9 (also known as Nercc1) (26, 27, 29). Nek2 is the most closely related mammalian kinase to NIMA and Fin1 by sequence and has been studied in the most detail. It localizes to the centrosome, where it phosphorylates and thereby regulates the association of a number of large coiled-coil proteins implicated in centrosome cohesion and microtubule anchoring (1, 10, 11, 21, 22, 30). These activities facilitate the early stages of spindle assembly at the G_2/M transition. Interestingly, *Aspergillus* NIMA and fission yeast Fin1 also localize to the fungal equivalent of the centrosome, namely the spindle pole body (15, 20, 38). Here, they may participate in positive feedback loops that promote the activation of Cdk1/cyclin B and mitotic entry.

Nek6, Nek7, and Nek9 act together in a mitotic kinase cascade, with Nek9 being upstream of Nek6 and Nek7. Nek9 was identified as an interacting partner of Nek6 and subsequently shown to phosphorylate Nek6 at S206 within its activation loop (2, 33). Both Nek9 and Nek6 have been reported to be activated in mitosis (2, 33, 39), although other studies dispute this (18, 23). NIMA-related kinases are characterized by having a conserved N-terminal catalytic domain, followed by a nonconserved C-terminal regulatory domain that varies in size and structure. Nek6 and Nek7 are significant exceptions to this, in that they are the smallest of the kinases and consist only of a catalytic domain with a very short N-terminal extension. They share significant similarity with each other, being 87% identical within their catalytic domains. Hence, although they exhibit distinct tissue expression patterns (8), it has generally been assumed that they are likely to have very similar properties and functions, with both being downstream substrates of Nek9.

* Corresponding author. Mailing address: Department of Biochemistry, University of Leicester, Lancaster Road, Leicester LE1 9HN, United Kingdom. Phone: 44 116 229 7069. Fax: 44 116 229 7018. E-mail: amf5@le.ac.uk.

§ Supplemental material for this article may be found at http://mcb.asm.org/.

▽ Published ahead of print on 4 May 2009.

Functional studies of Nek9 reveal that it has major roles to play in the organization of the mitotic spindle. Expression of inactive and truncated Nek9 mutants led to the missegregation of chromosomes, while injection of anti-Nek9 antibodies into prophase cells caused aberrant mitotic spindle formation (33). Similarly, depletion of Nek9 from *Xenopus* egg extracts led to a reduction in the formation of bipolar spindles in vitro (32; J. Blot and A. M. Fry, unpublished results). The basis for these defects remains unclear, but a number of binding partners have been identified that suggest possible functions in microtubule nucleation and anchoring, including components of the γ-tubulin ring complex (γ-TuRC), the Ran GTPase, and BicD2 (18, 32, 33).

While Nek9 is proposed to act upstream of Nek6 and Nek7, the proportion of its activities being channeled through these kinases is not known. Limited studies have been performed by looking at the consequences of expressing kinase-inactive Nek6 or Nek7 constructs or depleting the proteins by RNA interference (RNAi). Interference with Nek6 has been reported by one group to lead to metaphase arrest and apoptosis (39), although this is disputed by another study (23). Interference with Nek7 apparently leads to an increase in the mitotic index and apoptosis (19, 40). A decrease in centrosome-associated γ-tubulin and microtubule nucleation was also detected upon RNAi of Nek7, which is interesting in light of the interaction between Nek9 and γ-tubulin. Furthermore, defects in cytokinesis were found upon Nek7 depletion if cells were allowed to progress past the spindle checkpoint by codepletion of Mad2 (19). Importantly, both Nek9 and Nek7 localize to centrosomes, further supporting the model that this is a major site of action for this family of kinases in spindle formation (19, 32, 40).

In this study, we set out to clarify the mitotic roles of Nek6 and Nek7 by examining the consequences of expression of mutants with different levels of kinase activity as well as depletion of the proteins by RNAi. Our results demonstrate that Nek6 and Nek7 are both activated in mitosis and that interference with either kinase leads to apoptosis following mitotic arrest. Interestingly, expression of inactive mutants or small interfering RNA (siRNA)-mediated depletion leads to a metaphase delay with fragile mitotic spindles, whereas expression of hypomorphic mutants or depletion in the presence of a spindle assembly checkpoint (SAC) inhibitor leads to an accumulation of cells in cytokinesis. Based on additional localization data, we propose that these kinases regulate microtubule organization not only at spindle poles but also within the mitotic spindle itself and possibly at the central spindle during late mitosis. This study therefore provides important novel insights into how Nek6 and Nek7 contribute to distinct molecular events in mitotic progression.

MATERIALS AND METHODS

Plasmid construction and mutagenesis. Full-length expressed sequence tags containing human Nek6 (3640103) and human Nek7 (IOH45126) were obtained from MRC Geneservice (United Kingdom) and Invitrogen (Paisley, United Kingdom), respectively. These were sequenced, and the open reading frames (146-1087 and 47-995, respectively) were amplified by PCR and inserted into the appropriate expression vectors. Vectors used were pcDNA-DEST53 (Invitrogen), pFLAG-CMV2 (Sigma, Poole, United Kingdom), and pCMV-Tag 3C (Stratagene, La Jolla, CA). Nek6 and Nek7 mutants were generated by PCR-based mutagenesis using the GeneTailor site-directed mutagenesis system (Invitrogen), with pFLAG-CMV2-Nek6 or pCDNA-DEST53-Nek6 and pFLAG-CMV2-Nek7 or pCDNA-DEST53-Nek7, respectively. All constructs were confirmed by DNA sequencing in-house or by Lark Technologies (Takeley, United Kingdom).

Antibody generation. For the production of Nek6 and Nek7 antibodies, rabbits were immunized with peptides from the distinct N-terminal regions of the Nek6 (residues 1 to 15) and Nek7 (residues 12 to 28) proteins coupled via an N-terminal cysteine to keyhole limpet hemocyanin. Sera were screened by Western blotting of HeLa cell lysates and immunofluorescence microscopy of methanol-fixed HeLa cells. Antibodies were affinity purified using the same Nek6 or Nek7 peptides covalently bound to a CNBr-activated Sepharose column, made according to the manufacturer's instructions (Amersham, Little Chalfont, United Kingdom). Columns were washed extensively with 10 mM Tris-HCl (pH 7.5), followed by 10 mM Tris-HCl (pH 7.5), 500 mM NaCl, and specific antibodies eluted with 100 mM glycine (pH 2.5) into tubes containing neutralizing quantities of 1 M Tris-HCl (pH 8.0).

Cell culture, synchronization, and transfection. HeLa and HEK 293 cells were grown in Dulbecco's modified Eagle's medium (DMEM; Invitrogen) supplemented with 10% heat-inactivated fetal bovine serum (FBS), 100 IU/ml penicillin, and 100 μg/ml streptomycin at 37°C in a 5% CO_2 atmosphere. RPE1-hTERT cells were grown in DMEM-F12 medium (Invitrogen) supplemented with 10% FBS, 100 IU/ml penicillin, 100 μg/ml streptomycin, and 75% $NaHCO_3$ at 37°C in a 5% CO_2 atmosphere. M phase-arrested cells were prepared by 16 h of treatment with 50 ng/ml nocodazole; rounded mitotic cells were collected by gently pipetting off the floating population. To prepare cells arrested in S phase, 1 mM hydroxyurea was added for 24 h. Synchronization was confirmed by flow cytometry. Transient transfections were performed with Lipofectamine 2000 reagent (Invitrogen), according to the manufacturer's instructions. To bypass the SAC, cells were treated with the Aurora B kinase inhibitor ZM447439 (Tocris Bioscience, Bristol, United Kingdom) at a concentration of 2 μM.

Generation of stable cell lines. Stable cell lines were generated by transfecting the relevant construct into a 10-cm dish of HeLa cells. After 24 h, cells were washed and incubated in selective media containing Geneticin (Invitrogen) until foci containing ~50 to 100 cells were detected (~3 to 4 weeks). Culture dishes were then washed with 1× phosphate-buffered saline (PBS) before foci were picked using paper cloning discs (Sigma). Each disk was soaked in 1× PBS containing 0.5 mM EDTA and then incubated over the foci for 5 to 10 min at 37°C. Discs were then transferred to individual wells of a 24-well plate, and cells were grown in selective media to allow attachment to the culture vessel. Cloning discs were then removed, and individual clones were expanded in selective media.

Fluorescence microscopy and live-cell imaging. Cells grown on acid-etched glass coverslips were fixed and permeabilized using ice-cold methanol and immunofluorescence microscopy or time-lapse imaging, carried out as previously described (17). Where indicated, cells were preextracted with extraction buffer {0.5% Triton X-100, 80 mM PIPES [piperazine-*N*,*N*′-bis(2-ethanesulfonic acid)] [pH 6.8], 1 mM $MgCl_2$, 1 mM EGTA} for 30 s prior to methanol fixation. Primary antibodies used were against Nek6 (2 μg/ml), γ-tubulin (0.15 μg/ml; Sigma), α-tubulin (0.3 μg/ml; Sigma), Flag (0.5 μg/ml; Sigma), green fluorescent protein (GFP) (0.25 μg/ml; Abcam, Cambridge, United Kingdom), and cleaved caspase 3 (1/100 dilution; Cell Signaling Technology, Danvers, MA). The secondary antibodies used were Alexa Fluor 488 and 594 goat anti-rabbit and goat anti-mouse immunoglobulin Gs (IgGs) (1 μg/ml; Invitrogen). Quantitative imaging was performed by capturing images with a TE300 inverted microscope (Nikon, United Kingdom) using an ORCA ER charge-coupled-device camera (Hamamatsu, Hamamatsu, Japan) and Openlab 5 software (Improvision, United Kingdom) and measuring the mean pixel intensity under nonsaturating exposure conditions with Openlab or ImageJ software within a fixed region of interest. Background readings were taken from appropriate neighboring regions of the image and subtracted from intensity measurements.

Immunoprecipitation and kinase assays. Cells were harvested by incubation with 1× PBS containing 0.5 mM EDTA and pelleted by centrifugation prior to being lysed in NEB lysis buffer (11). Lysates were immunoprecipitated using antibodies against purified Nek6 (2 μg/ml), Nek7 (2 μg/ml), or Flag (0.5 μg/ml; Sigma). Kinase assays were carried out using either 5 to 10 μl of washed immune complex beads prepared as described above or 0.1 μg purified kinase (Millipore, Watford, United Kingdom). Proteins were incubated with 5 μg of β-casein or purified bovine microtubules (Cytoskeleton Inc.) and 1 μCi of [γ-^{32}P]ATP in 40 μl kinase buffer (50 mM HEPES · KOH [pH 7.4], 5 mM $MnCl_2$, 5 mM β-glycerophosphate, 5 mM NaF, 4 μM ATP, 1 mM dithiothreitol) at 30°C for 30 min. Reactions were stopped with 50 μl of protein sample buffer and analyzed by sodium dodecyl sulfate-polyacrylamide gel electrophoresis (SDS-PAGE) and

autoradiography. Substrate phosphorylation was quantified by scintillation counting of proteins excised from dried gels.

RNAi. siRNA oligonucleotides specific to Nek6 (GAUCGAGCAGUGUGA CUACdTdT) or Nek7 (CTCCGACAGTTAGTTAATATTdTdT) were obtained from Ambion (Austin, TX) and transfected into HeLa cells using siPORT-NeoFX transfection reagent (Ambion), according to the manufacturer's instructions. A total of 72 h after transfection, cells were either fixed for immunocytochemistry or prepared for Western blot or flow cytometry analysis.

Apoptosis assays and flow cytometry. Apoptosis was determined by annexin V/fluorescein isothiocyanate (FITC) binding and flow cytometry (Bender MedSystems GmbH, Vienna, Austria) or by cleaved caspase 3 staining. For flow cytometry, cells were harvested by incubation with 1× PBS containing 0.5 mM EDTA before being resuspended in 10 ml DMEM supplemented with 10% FBS, 100 IU/ml penicillin, and 100 μg/ml streptomycin and allowed to recover at 37°C in a 5% CO_2 atmosphere for 1 h. Cells were then stained with annexin V/FITC in annexin binding buffer (10 mM HEPES [pH 7.4], 140 mM NaCl, 2.5 mM $CaCl_2$) for 10 min at room temperature before being washed in annexin binding buffer and resuspended in binding buffer supplemented with 1 μg/ml propidium iodide. To determine cell cycle distribution, cells were harvested and fixed in ice-cold 70% ethanol for 30 min at 4°C. Cells were washed twice in 1× PBS and resuspended in 1× PBS containing 2.5 μg/ml RNase A and 5 μg/ml propidium iodide. Cells were analyzed via flow cytometry, using a FACScan II instrument and CellQuest Pro software (BD Biosciences, San Jose, CA). To block apoptosis, zVAD-fmk (100 μM; MP Biomedical) was added to the cell culture medium.

Miscellaneous techniques. Preparation of cell extracts, SDS-PAGE, and Western blotting were performed as previously described (17). For Western blotting, primary antibodies used were against Nek6 (1 μg/ml), Nek7 (1 μg/ml), Nek9 (1.5 μg/ml; Abcam), α-tubulin (0.3 μg/ml; Sigma), Flag (0.5 μg/ml; Sigma), and GFP (0.25 μg/ml; Abcam). Secondary antibodies used were alkaline phosphatase-conjugated anti-rabbit or anti-mouse IgGs (1:7,500 dilution; Promega, Southampton, United Kingdom) or horseradish peroxidase-labeled secondary antibodies (Amersham). Microtubule sedimentation assays using purified (>99% purity) bovine microtubules (Cytoskeleton Inc.) were also performed as previously described (17).

RESULTS

Kinase-inactive Nek6 and Nek7 mutants induce apoptosis. Expression of a Nek6 construct with mutations in two adjacent sites within the ATP-binding pocket, K74 and K75, induced mitotic arrest and apoptosis in HeLa cells, although it was not shown which of these sites is critical (39). Similarly, mutation of G43 in the Nek7 kinase subdomain I caused a small increase in apoptosis in HeLa cells, although no direct measurement of the kinase activity for this mutant was shown (40). However, it was separately reported that expression of kinase-deficient Nek6 or Nek7 in NIH 3T3, U2OS, or HeLa cells does not interfere with cell cycle progression (23). To systematically determine whether mutants of human Nek6 and Nek7 with differing levels of kinase activity are capable of stimulating apoptosis and/or mitotic arrest, we first generated five mutants of each kinase, including single mutations of the lysines present in the ATP-binding pocket, a double mutation of these lysines, and single mutations of two putative phosphorylation sites in the activation loop. To compare the relative activities of these mutants, N-terminally Flag-tagged constructs were expressed in HEK 293 cells and immunoprecipitated with anti-Flag antibodies, and the activity was determined using β-casein as a substrate (Fig. 1A and B). Mutation of K75M in Nek6 (Nek6-K75M) and K64M in Nek7 (Nek7-K64M) led to an almost complete loss of activity (<5% compared to that of the wild type), whereas mutation of the adjacent K74M in Nek6 (Nek6-K74M) and K63M in Nek7 (Nek7-K63M) had very little effect on activity. The double lysine mutants (Nek6-K74M/K75M and Nek7-K63M/K64M) were inactive, as expected. With the activation loop mutants, Nek6-T202A and Nek7-T191A retained approximately 30 to 40% activity, whereas Nek6-S206A and Nek7-S195A retained only 10 to 15% activity. These latter results are in line with data published on the C-terminally myc/His-tagged Nek6 activation loop mutants (2).

Having determined the relative activity levels of these mutants, we then examined their ability to induce apoptosis in HeLa cells. This was determined by both flow cytometric counting of annexin V staining (Fig. 1C) and microscopic observation of cleaved caspase 3 staining (Fig. 1D). Expression of wild-type Nek6 or Nek7 induced an increase by approximately twofold in apoptosis (~10% of cells) compared to that of control transfections (~5% of cells). Similarly, the Nek6-K74M and Nek7-K63M mutants that retained almost full activity also caused only a modest increase in apoptosis. However, the inactive mutants Nek6-K75M and Nek7-K64M induced apoptosis in 40 to 70% of cells. The activation loop mutants that retained the least activity, Nek6-S206A and Nek7-S195A, also led to substantial levels of apoptosis (45 to 70%), whereas the activation loop mutants with partial activity, Nek6-T202A and Nek7-T191A, led to intermediate levels of apoptosis (30 to 35%). This graded induction of apoptosis was also seen in the immortalized, but nontransformed, RPE1-hTERT cells (Fig. 1E). Hence, the extent of apoptosis is inversely related to the relative activity of the Nek6 or Nek7 protein.

To determine whether induction of apoptosis was dependent upon cell cycle status, cells transiently expressing wild-type Nek6 or the inactive Nek6-K75M mutant were either untreated or treated with nocodazole to arrest cells in mitosis (Fig. 1F) or with hydroxyurea to arrest cells in S phase (Fig. 1G). Of the cells expressing the Nek6-K75M mutant, those that were untreated or arrested in mitosis underwent substantial levels of apoptosis, whereas those blocked in S phase did not, demonstrating that apoptosis is most likely dependent upon mitotic entry.

Nek6- and Nek7-inactive mutants delay cells at metaphase and cytokinesis. Immunofluorescence microscopy of cells expressing kinase-inactive Nek6 or Nek7 mutants revealed that many cells that stained positively for the apoptotic marker cleaved caspase 3 also exhibited features of mitotic cells, such as the alignment of chromosomes on a metaphase plate or segregation of masses of DNA (Fig. 2A to C). This falls in line with our data showing that apoptosis depends upon mitotic entry and with the report of Yin et al. (39) showing that apoptosis in cells expressing kinase-inactive Nek6 follows mitotic arrest. To determine whether the different Nek6 and Nek7 mutants caused a mitotic delay, HeLa cells were transfected with Flag-tagged constructs and analyzed by immunofluorescence microscopy after 24 h and before significant levels of apoptosis had occurred. First, it was seen that wild-type Nek6 and Nek7, as well as the Nek6-K74M and Nek7-K63M mutants that retain almost full activity, caused a moderate increase (by three- to fourfold) in the number of cells in metaphase (Fig. 2D). However, the inactive mutants Nek6-K75M and Nek7-K64M caused a more substantial increase (by seven- to ninefold) in the number of cells in metaphase. Intriguingly, the activation loop mutants with 30 to 40% activity, Nek6-T202A and Nek7-T191A, predominantly exhibited a late mitotic delay phenotype, with an increase of 5- to 10-fold in cells that had passed metaphase but not completed cytokinesis. The

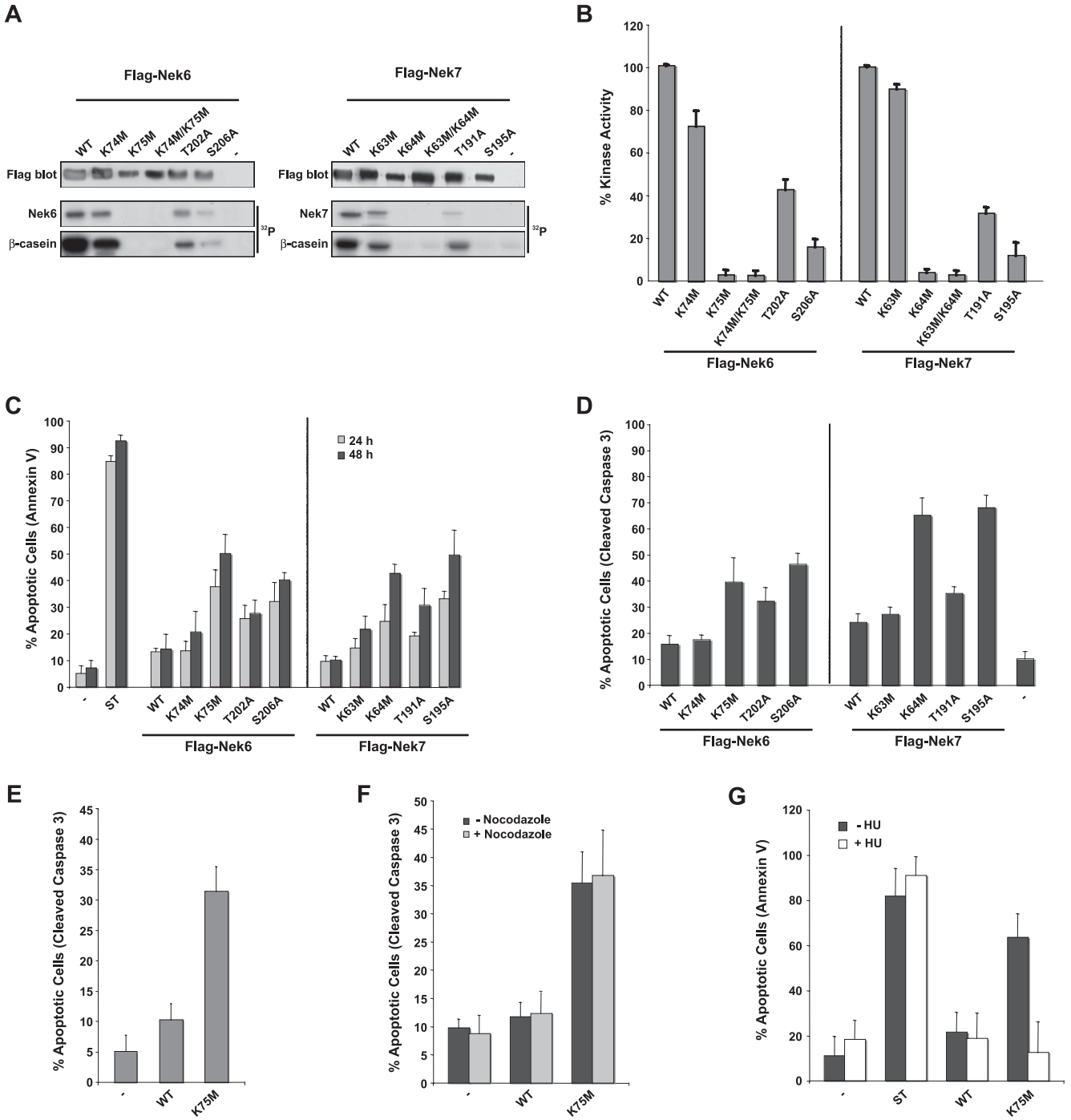

FIG. 1. Expression of kinase-inactive Nek6 and Nek7 mutants induces apoptosis. (A) HEK 293 cells were transiently transfected with FLAG-tagged Nek6 and Nek7 constructs, as indicated, for 24 h before cells were lysed and subjected to immunoprecipitation with anti-Flag antibodies. The amount of kinase precipitated was determined by Western blotting with anti-Flag antibodies and the immunoprecipitates used for kinase assays, with β-casein as a substrate. Autoradiographs (^{32}P) are shown of the Nek6/Nek7 and β-casein proteins. WT, wild type. (B) Activity of the different Nek6 and Nek7 constructs is expressed as a percentage of wild-type activity normalized to the amount of precipitated protein. The data are shown as means ± standard deviations from three separate experiments. (C) HeLa cells were transiently transfected with Flag-tagged Nek6 and Nek7 constructs for 24 and 48 h before being assayed for their ability to take up annexin V/FITC stain via flow cytometry analysis. As a positive control, untransfected cells were treated with 1 μM staurosporine (ST) for 4 h. (D) HeLa cells were transiently transfected with Flag-tagged Nek6 and Nek7 constructs for 48 h before being fixed and stained with Flag antibodies to detect transfected cells and cleaved caspase 3 antibodies to detect apoptotic cells. Data in panels C and D represent means (±standard deviations) from counts of at least 50 cells in three separate experiments. (E) RPE1-hTERT cells were transiently transfected with FLAG-tagged Nek6-WT and Nek6-K75M constructs for 48 h before being fixed and stained with anti-FLAG and anti-cleaved caspase 3 antibodies. Data represent means (±standard deviations) from counts of at least 100 cells in three separate experiments. (F) HeLa cells were transiently transfected with FLAG-tagged Nek6-WT and Nek6-K75M constructs for 48 h with and without treatment with 500 ng/ml nocodazole before being fixed and stained with anti-FLAG antibodies to detect transfected cells and anti-cleaved caspase 3 antibodies to detect apoptotic cells. Data represent means (±standard deviations) from counts of at least 100 cells in three separate experiments. (G) HeLa cells were transiently transfected with Flag-Nek6 constructs for 48 h in the presence or absence of 1 mM hydroxyurea before being assayed for their ability to take up annexin V/FITC via flow cytometry analysis. Data represent means (±standard deviations) from three separate experiments. In all experiments, untransfected cells (−) were used as a negative control.

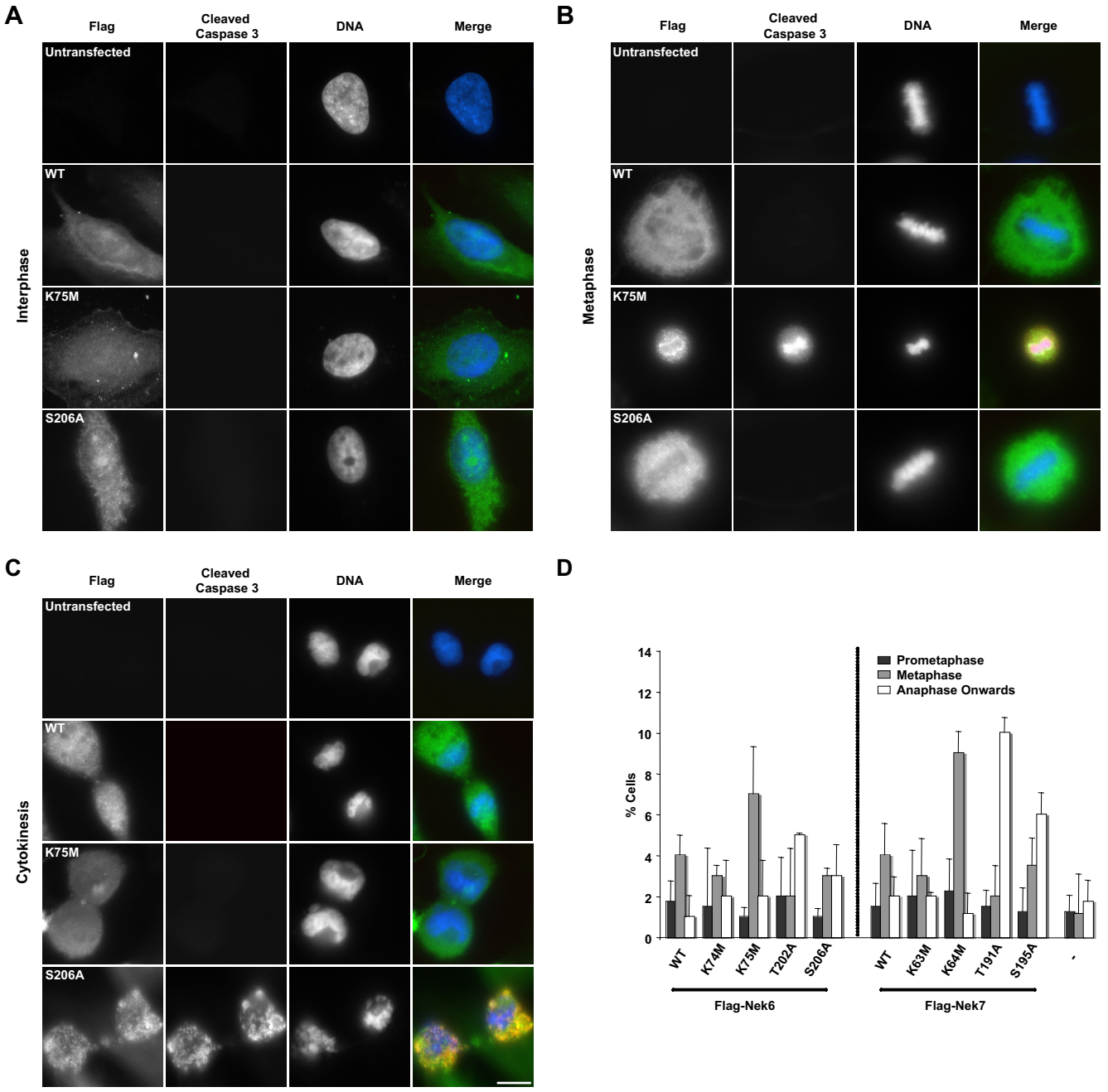

FIG. 2. Kinase-inactive Nek6 and Nek7 trigger mitotic delay at two stages. (A to C) HeLa cells were either untransfected or transfected, as indicated, with Flag-tagged Nek6-wild type (WT), Nek6-K75M, or Nek6-S206A for 48 h before being fixed and stained with antibodies against Flag (green in merge) to detect transfected cells and cleaved caspase 3 (red in merge) to detect apoptotic cells. DNA was stained with Hoechst 33258 (blue in merge). Cells in interphase (A), metaphase (B), and cytokinesis (C) are shown. Scale bar, 10 μm. (D) HeLa cells were either untransfected (−) or transiently transfected with different Flag-Nek6 and Flag-Nek7 constructs, as indicated, for 24 h before being processed for immunofluorescence microscopy with Flag antibodies to detect transfected cells and α-tubulin antibodies to detect the mitotic spindle. The histogram represents the observed frequency of transfected cells in the different stages of mitosis indicated. Data are means (±standard deviations) from three separate experiments, in which at least 50 cells were counted for each construct.

Nek6-S206A and Nek7-S195A mutants that had partial activity exhibited an intermediate phenotype, with increases in both metaphase and late mitotic populations. Thus, mutants with little or no activity block cells in metaphase, whereas those that have partial activity, which we refer to as hypomorphic mutants, progress beyond metaphase but delay in late mitosis.

It has been previously shown that human MDA-MB-231 breast cancer cells stably expressing the Nek6-K74M/K75M double mutant can be generated but exhibit a reduced growth rate (39). We therefore attempted to generate HeLa cells stably expressing GFP-tagged wild-type and mutant Nek6 and Nek7 proteins that could be used for time-lapse studies of

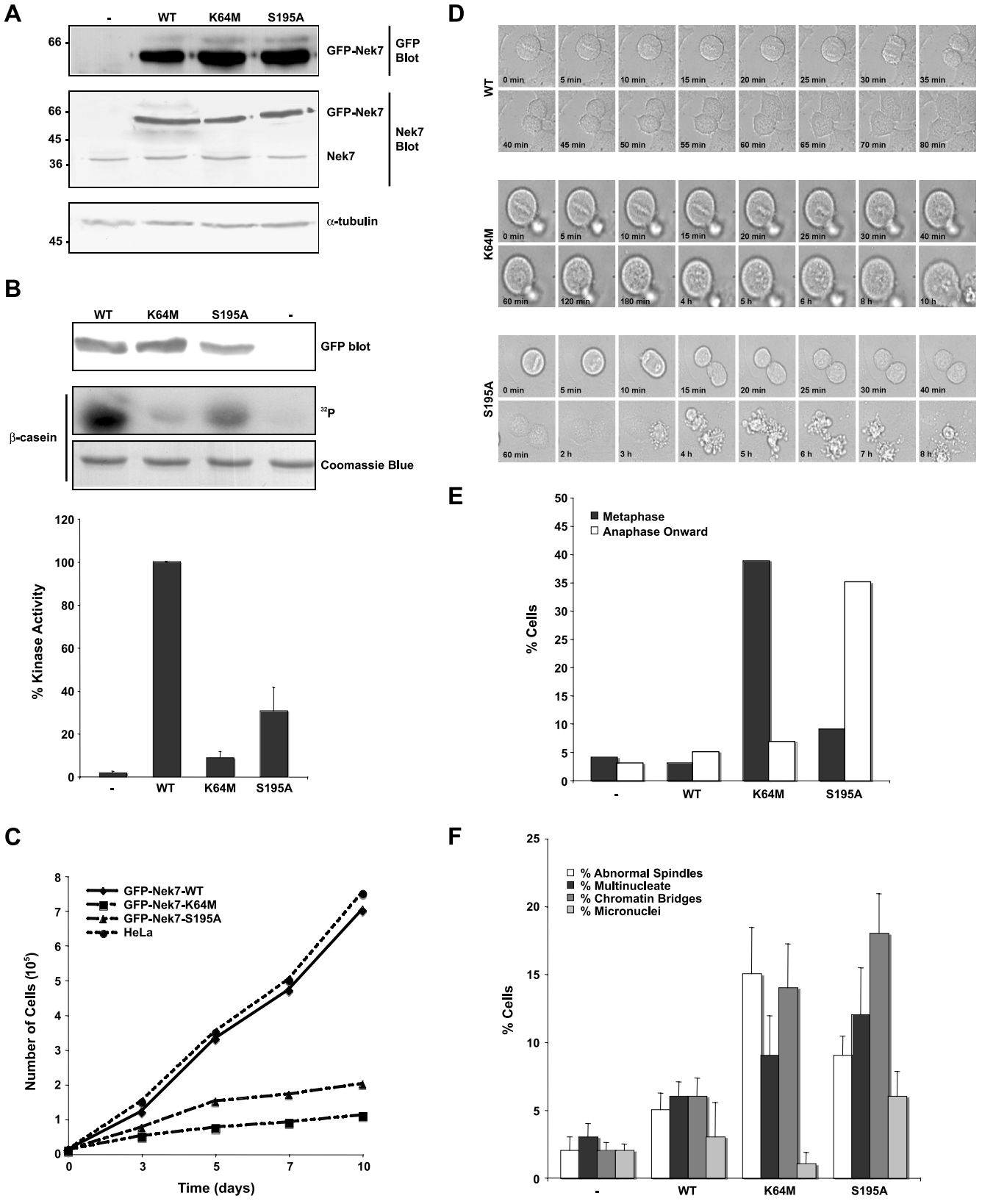

FIG. 3. Cells stably expressing kinase-inactive Nek7 exhibit defective cell cycle progression. (A) Cell lysates were prepared from parental HeLa cells (−) or HeLa cells stably expressing GFP-Nek7 constructs, as indicated, and were subjected to SDS-PAGE and Western blot analysis with antibodies against GFP, Nek7, and α-tubulin. Molecular masses (kDa) are indicated on the left. WT, wild type. (B) Cell lysates were subjected to immunoprecipitation with anti-GFP antibodies, as described in the legend for Fig. 1A. The amount of kinase precipitated was determined by Western blotting with anti-GFP antibodies and the immunoprecipitates used for kinase assays, with β-casein as a substrate. Products were analyzed

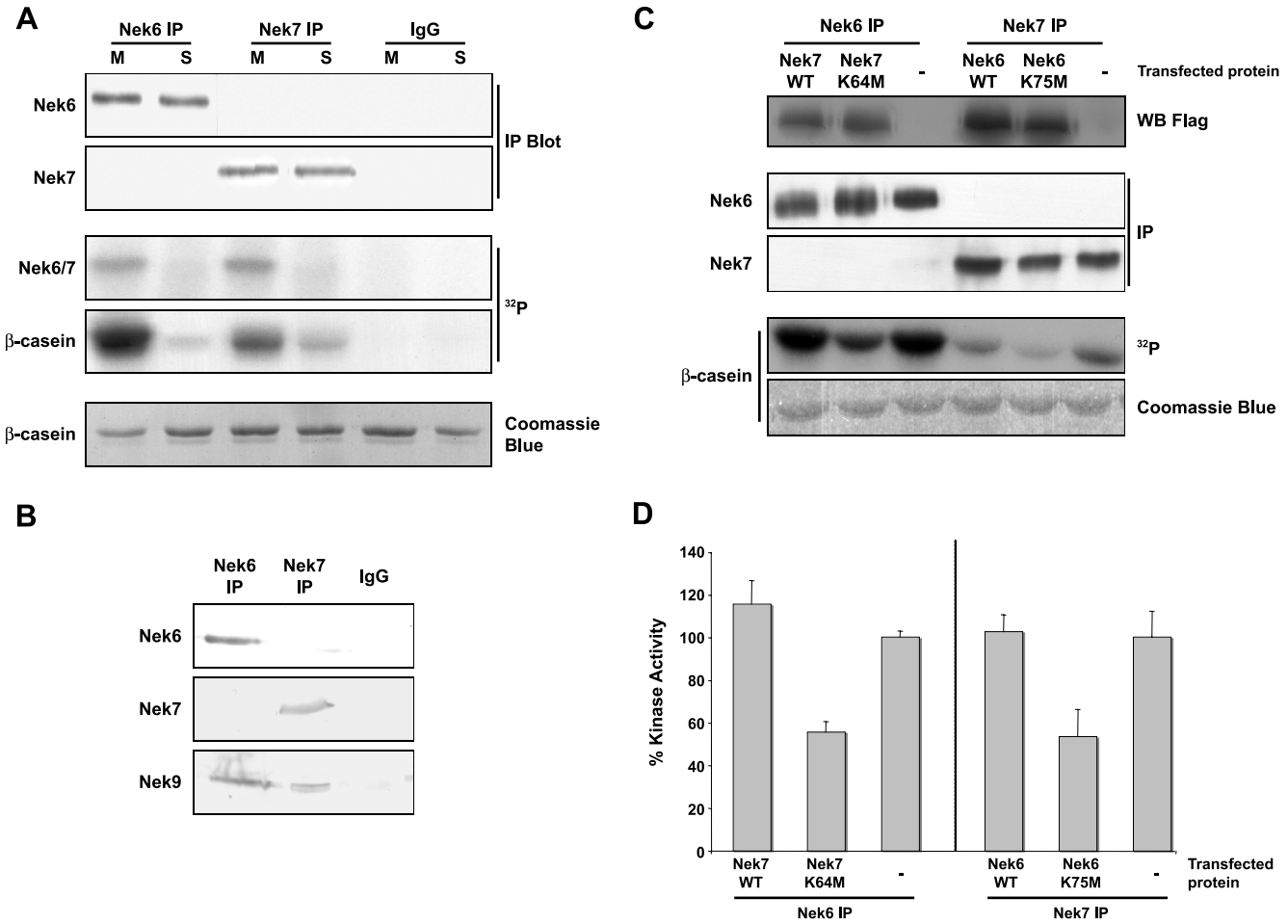

FIG. 4. Endogenous Nek6 and Nek7 are activated in mitosis. (A) Lysates were prepared from untransfected HEK 293 cells synchronized in S or M phase of the cell cycle with hydroxyurea or nocodazole, respectively, and proteins immunoprecipitated with Nek6 or Nek7 antibodies or control rabbit IgGs. The immunoprecipitates were subjected to Western blotting (IP blot) with Nek6 or Nek7 antibodies and used in kinase assays, with β-casein as a substrate. Samples were analyzed by SDS-PAGE, Coomassie blue staining, and autoradiography (^{32}P). (B) Lysates were prepared from untransfected, asynchronous HEK 293 cells and proteins immunoprecipitated with Nek6 or Nek7 antibodies or control rabbit IgGs. Immunoprecipitates were subjected to Western blotting with Nek6, Nek7, or Nek9 antibodies. (C) HEK 293 cells were either untransfected (−) or transiently transfected with Flag-Nek7-wild type (WT) or Flag-Nek7-K64M and Flag-Nek6-WT or Flag-Nek6-K75M constructs, as indicated. After 24 h, cells lysates were subjected to Western blotting with Flag antibodies to determine transfection efficiency. Lysates were subjected to immunoprecipitation (IP) with Nek6 or Nek7 antibodies and immunoprecipitates used for Western blot analysis and kinase assays, with β-casein as a substrate. Samples were analyzed by SDS-PAGE, Coomassie blue staining, and autoradiography (^{32}P). (D) Activity levels of the immunoprecipitated proteins are expressed as a percentage of wild-type activity in untransfected (−) cells normalized to the amount of precipitated protein. The data are shown as means (±standard deviations) from three separate experiments.

mitotic progression. In our case, no Nek6 stable clones could be isolated, but rather surprisingly in light of the transient transfection results, we were able to isolate rare clones expressing wild-type Nek7 as well as the Nek7-K64M and Nek7-S195A mutants (Fig. 3A). These GFP-tagged proteins showed similar levels of activity when immunoprecipitated from HeLa cells to the Flag-tagged proteins expressed in HEK 293 cells (compare Fig. 3B to 1B). As predicted from our transient expression

by SDS-PAGE, Coomassie blue staining, and autoradiography (^{32}P). Activity levels of the different Nek7 constructs are expressed as a percentage of the wild-type activity normalized to the amount of precipitated protein. The data are shown as means (±standard deviations) from three separate experiments. (C) Growth curves of HeLa cells stably expressing GFP-Nek7 constructs are shown; data represent the means from three separate experiments. (D) Mitotic HeLa cells stably expressing GFP-Nek7 constructs, as indicated, were analyzed by time-lapse bright-field microscopy. Images are presented from metaphase onwards, with time indicated on each panel. (E) The outcome of each live cell imaged as in panel D was scored according to whether they were delayed in metaphase or late mitosis prior to undergoing apoptosis or whether they progressed normally. A total of 40 to 50 cells were scored for each cell line. (F) Parental HeLa cells (−) or HeLa cells stably expressing GFP-Nek7 proteins, as indicated, were fixed and stained with α-tubulin antibodies to detect the microtubule network and Hoechst 33258 to detect DNA. The percentage of cells with abnormal mitotic spindles or cells that were multinucleated, micronucleated, or still attached by chromatin bridges was scored. Data represents means (±standard deviations) from counts of at least 150 cells in three independent experiments.

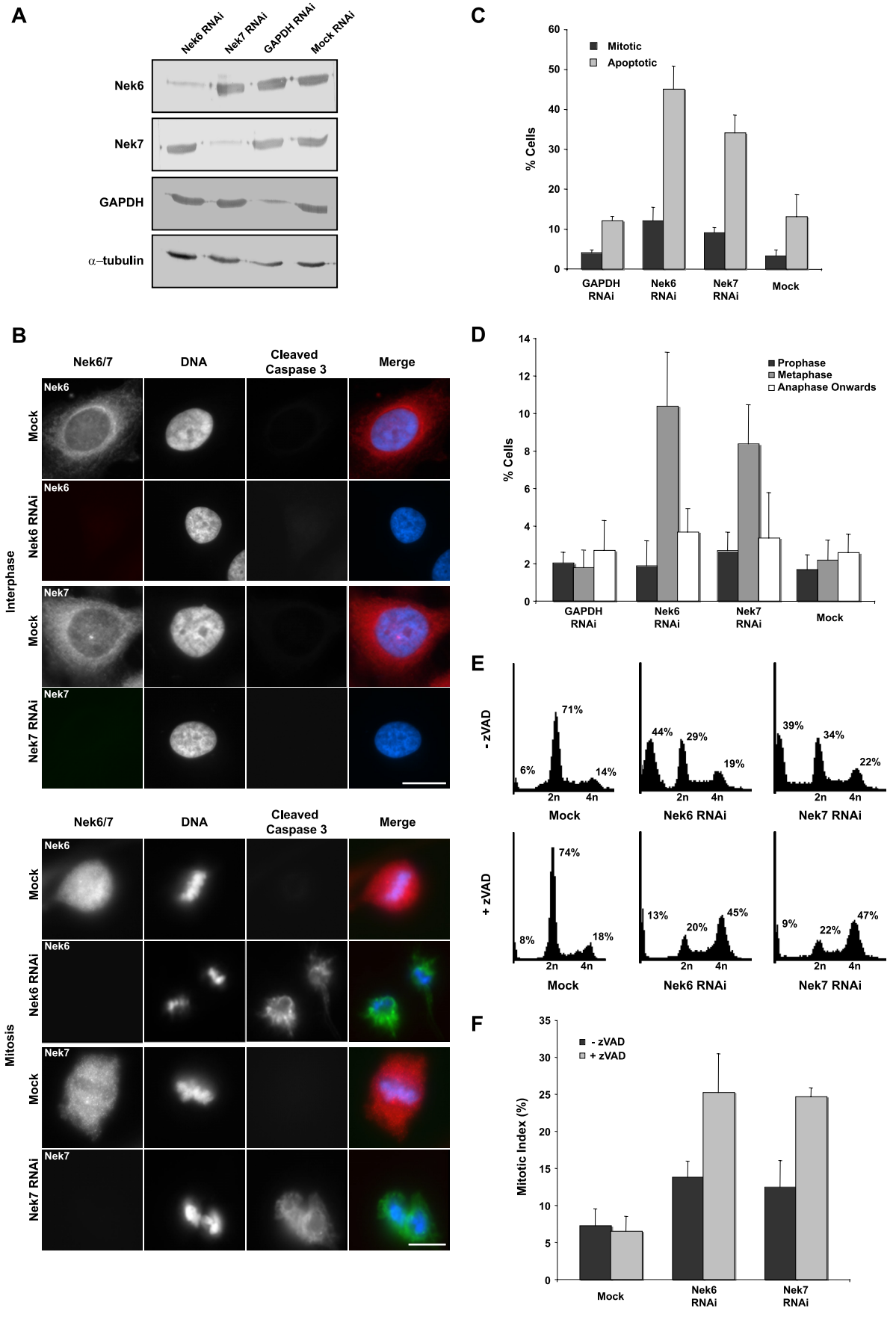
A
Nek6 RNAi
Nek7 RNAi
GAPDH RNAi
Mock RNAi
Nek6
Nek7
GAPDH
α–tubulin
B
Nek6/7
DNA
Cleaved Caspase 3
Merge
Interphase
Mock
Nek6 RNAi
Nek7 RNAi
Nek6
Nek7
Mitosis
C
Mitotic
Apoptotic
% Cells
GAPDH RNAi
Nek6 RNAi
Nek7 RNAi
Mock
D
Prophase
Metaphase
Anaphase Onwards
% Cells
E
- zVAD
+ zVAD
6%
71%
14%
44%
29%
19%
39%
34%
22%
8%
74%
18%
13%
20%
45%
9%
22%
47%
2n
4n
Mock
Nek6 RNAi
Nek7 RNAi
F
- zVAD
+ zVAD
Mitotic Index (%)
Mock
Nek6 RNAi
Nek7 RNAi

studies, these cell lines were difficult to maintain for any length of time, and those expressing the Nek7-K64M or Nek7-S195A mutants exhibited severely impaired growth rates (Fig. 3C). We then analyzed these cells by phase contrast time-lapse microscopy, selecting cells that had reached metaphase for imaging to avoid potential photoactivation of DNA damage checkpoints in early mitosis. Whereas cells expressing wild-type Nek7 entered anaphase within 20 to 30 min and exited mitosis within 1 to 2 h, 40% of cells expressing the inactive Nek7-K64M remained arrested in metaphase for many hours before eventually undergoing apoptosis (Fig. 3D and E). During this time, the chromosomes lost their alignment on the metaphase plate and became less distinct. In contrast, only 10% of cells expressing the hypomorphic Nek7-S195A mutant were delayed at the metaphase-anaphase transition. However, 35% of cells initiated an exit from mitosis but were unable to complete cytokinesis, eventually undergoing apoptosis (Fig. 3D and E). Furthermore, counts of fixed cells revealed that the Nek7-S195A cell line exhibited the highest frequencies of multinucleated and micronucleated cells and cells still connected by chromatin bridges (35%), more than the Nek7-K64M cell line (25%) or the wild-type cell line (15%) (Fig. 3F). This is consistent with the S195A mutation allowing cells to progress through metaphase but interfering with the completion of cytokinesis.

Nek6 and Nek7 are activated in mitosis, and depletion leads to mitotic delay and apoptosis. It has been reported by two groups that Nek6 is activated in mitosis (2, 39), but this was disputed by a third group (23). No data have yet been published on Nek7 activity through the cell cycle. We therefore raised polyclonal antibodies to peptides derived from the distinct N-terminal extensions that Western blotting recognized as single bands at the predicted sizes that disappeared upon RNAi depletion (Fig. 4A and 5A). They also detected only the appropriate recombinant proteins (Fig. 4C). These were then used to immunoprecipitate the proteins from S or M phase drug-arrested HeLa cells, and the activity was measured, using β-casein as a substrate. Both Nek6 and Nek7 were specifically autophosphorylated and activated in cells arrested in mitosis compared to cells arrested in S phase (Fig. 4A).

Nek6 is known to interact with Nek9, although such an interaction has not been reported for Nek7. We therefore probed Nek6 and Nek7 immunoprecipitates with Nek9 antibodies and found that, while both proteins coprecipitate Nek9, they do not coprecipitate each other, indicating that separate complexes of Nek6 with Nek9 and Nek7 with Nek9 exist in cells (Fig. 4B). We then measured the activity of endogenous Nek6 in cells expressing exogenous Nek7 proteins and vice versa. Interestingly, this experiment first revealed an apparently greater level of activity for endogenous Nek6 in cells than for Nek7 (Fig. 4C). However, as the relative avidity of the different antibodies for the two kinases and their ability to use β-casein as a substrate may differ, this conclusion would be premature. Second, the data showed that cells expressing kinase-inactive Nek6 had reduced the activity of endogenous Nek7 and vice versa (Fig. 4C and D). This indicates that the kinase-inactive mutants can interfere with the activity of both endogenous Nek6 and Nek7, most likely through titrating Nek9 into inactive complexes. As Nek9 may have additional substrates besides Nek6 and Nek7, this raises the possibility that some of the phenotypes that arise from expression of kinase-inactive Nek6 or Nek7 may be the result of interference with Nek9.

Therefore, to specifically examine the function of the individual kinases, we switched to using RNAi-mediated depletion. Depletion of Nek6 or Nek7 has been reported to induce mitotic arrest and apoptosis in a manner similar to that of overexpression of kinase-inactive proteins (19, 39, 40). We used siRNA oligonucleotides to specifically deplete Nek6, Nek7, or as a control, GAPDH (glyceraldehyde-3-phosphate dehydrogenase), in HeLa cells to <10% of the normal levels (Fig. 5A). Depletion of Nek6 or Nek7 had no effect on expression of the complementary kinase. Analysis by immunofluorescence microscopy for cleaved caspase 3 or flow cytometry for annexin V revealed that after 72 h of Nek6 or Nek7 depletion, 30 to 45% of cells were undergoing apoptosis (Fig. 5B and C). This suggests that the loss of Nek6 is not rescued by the presence of endogenous Nek7 and vice versa, meaning that the kinases cannot be redundant in HeLa cells. Moreover, fluorescence microscopy revealed an increase in the mitotic index (Fig. 5C) and a significant increase in the proportion of cells in metaphase (Fig. 5D). Confirmation that apoptosis follows mitotic delay was obtained by using flow cytometry to show that treatment of RNAi-depleted cells with the caspase inhibitor zVAD led to a substantial shift in the fraction of cells with sub-2n DNA content (apoptotic) to cells with 4n DNA content (G_2/M) (Fig. 5E). Mitotic index counts confirmed that the majority of these cells were in mitosis (Fig. 5F).

FIG. 5. RNAi depletion of Nek6 or Nek7 induces apoptosis following mitotic arrest. (A) HeLa cells were either mock transfected or transfected with siRNA oligonucleotides targeted against Nek6, Nek7, or GAPDH. After 72 h, extracts were prepared and analyzed by SDS-PAGE and Western blotting with Nek6, Nek7, GAPDH, or α-tubulin antibodies. (B) HeLa cells were transfected with siRNA oligonucleotides, as indicated, for 72 h before being fixed and analyzed by immunofluorescence microscopy with antibodies against Nek6 or Nek7 (red on merge) and cleaved caspase 3 (green on merge). DNA was stained with Hoechst 33258 (blue on merge). Cells in interphase and mitosis are shown. Scale bar, 10 μm. (C) HeLa cells were treated with siRNA oligonucleotides for 72 h, as indicated, and analyzed as described in the legend for panel B. A total of 100 to 300 cells were scored for mitosis or apoptosis in three independent experiments, and means (±standard deviations) are indicated. (D) Following treatment of cells with siRNA oligonucleotides, as indicated, the frequencies of cells in different stages of mitosis were scored. Data represent means (±standard deviations) from three separate experiments, counting at least 100 cells per experiment. (E) HeLa cells were transfected with Nek6 or Nek7 siRNA oligonucleotides or mock transfected for 72 h in the presence or absence of 100 μM zVAD, as indicated. Cells were then harvested and fixed before being stained with propidium iodide and before the cell cycle distribution being analyzed by flow cytometry. The percentages of cells in less than 2n, 2n, and 4n peaks are indicated. (F) HeLa cells were transfected with Nek6 or Nek7 siRNA oligonucleotides or mock transfected for 72 h in the presence or absence of zVAD before being fixed and analyzed by immunofluorescence microscopy, and the frequencies of cells in mitosis were scored. Data represent means (±standard deviations) from three separate experiments, counting at least 100 cells in each.

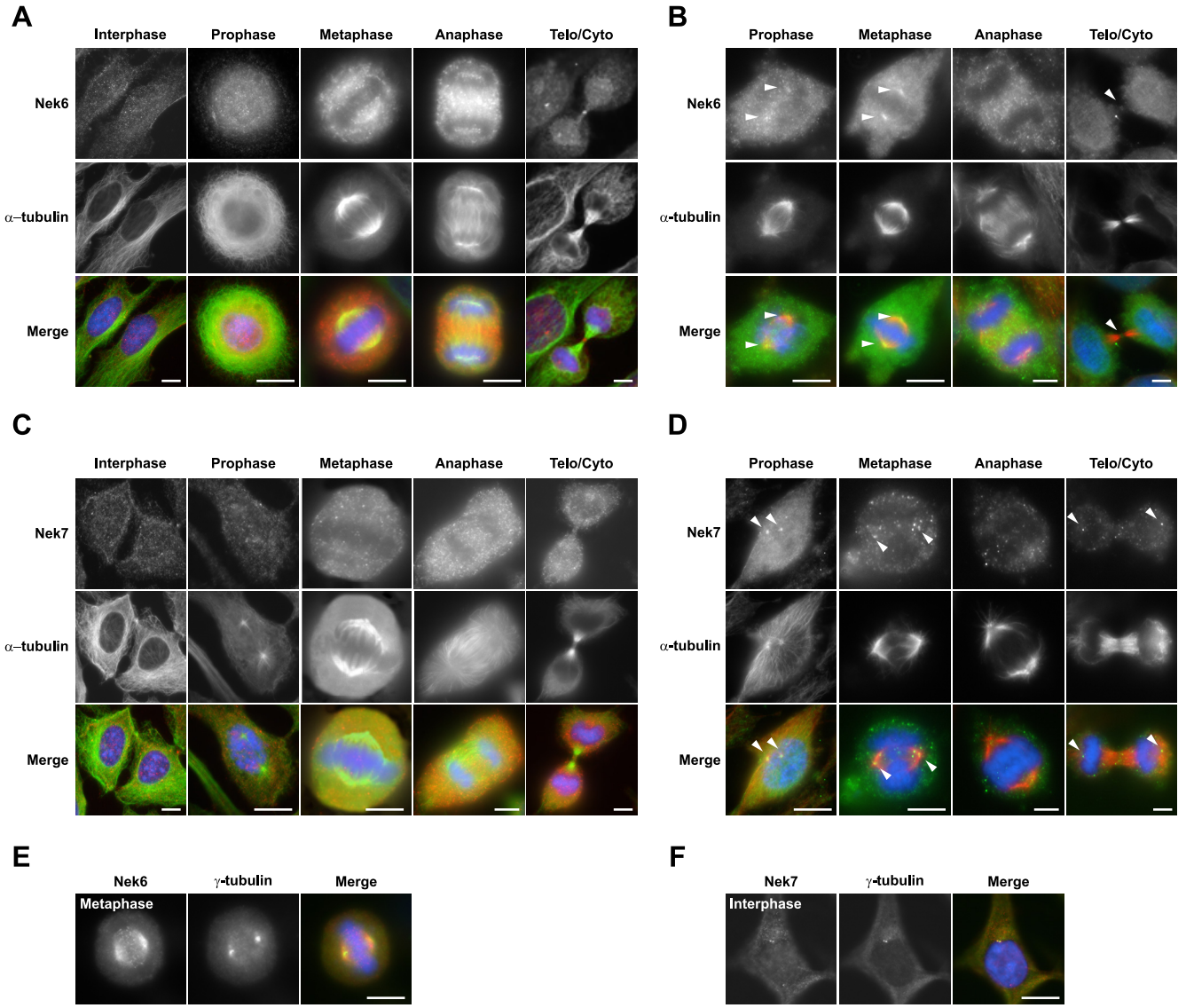

FIG. 6. In mitosis, Nek6 localizes to spindle microtubules and spindle poles, while Nek7 localizes only with spindle poles. (A) HeLa cells were processed for immunofluorescence microscopy with Nek6 (red in merge) and α-tubulin (green in merge) antibodies. Telo/Cyto, telophase/cytokinesis. (B) HeLa cells were treated with extraction buffer for 30 s before being fixed and permeabilized in methanol and processed for immunofluorescence microscopy, as described in the legend for panel A. Arrowheads denote spindle pole or midbody staining. (C and D) Same process as described in legends for panels A and B, respectively, except using Nek7 (red) antibodies. (E and F) HeLa cells were fixed and processed for immunofluorescence microscopy with Nek6 or Nek7 (red) antibodies, as indicated, and γ-tubulin (green) antibodies. In all panels, DNA was stained with Hoechst 33258 (blue), and merged images are shown. Scale bars, 10 μm.

Nek6 localizes to different microtubule-based structures in mitosis, whereas Nek7 is restricted to spindle poles. To determine whether endogenous Nek6 and Nek7 concentrate at spindle poles or indeed stain any other mitotic structures, we examined their subcellular localization using the specific antipeptide antibodies that we had previously verified for use in immunofluorescence microscopy by RNAi (Fig. 5B). In interphase cells, using standard methanol fixation, Nek6 and Nek7 were generally distributed in a diffuse manner throughout both the cytoplasm and the nucleus (Fig. 6A and C). Nek7 was detected at centrosomes in some interphase cells, but the majority did not show such colocalization, and analysis of synchronized cells did not suggest that this was cell cycle dependent (Fig. 6C and F). In mitotic cells, a fraction of Nek6 became detectable on the microtubules of the mitotic spindle in metaphase cells and of the central spindle in anaphase cells and at the midbody in cells undergoing cytokinesis (Fig. 6A and E). In contrast, Nek7 was not detected on any particular mitotic structure (Fig. 6C), and neither protein could be seen associated with spindle poles.

However, to more clearly see whether Nek6 or Nek7 associated with any particular mitotic structure, we preextracted cells with detergent prior to fixation (Fig. 6B and D). Importantly, this now revealed a fraction of both Nek6 and Nek7 at spindle poles in prophase and metaphase. Nek7, but not Nek6, could also be weakly detected at spindle poles in late mitotic

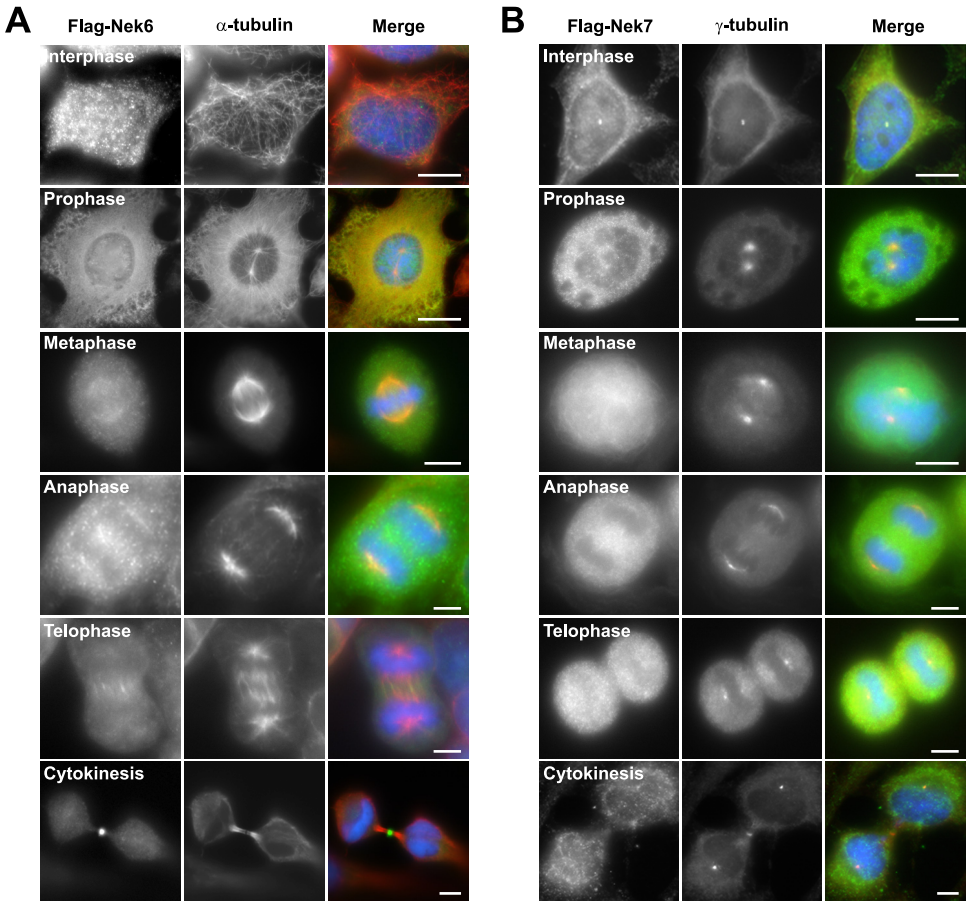

FIG. 7. HeLa cells were transiently transfected with Flag-tagged Nek6-wild type (A) or Nek7-wild type (B) constructs for 24 h before being processed for immunofluorescence microscopy with Flag (green in merge) and α-tubulin (red in merge) antibodies. DNA was stained with Hoechst 33258 (blue). Scale bars, 10 μm.

cells. Interestingly, in anaphase cells, Nek6 was again clearly seen in the vicinity of the central spindle, but after extraction, it was more obviously punctate in this region and highly reminiscent of microtubule plus ends.

One drawback with using single epitope-based peptide antibodies is that this epitope may be masked in cells under certain conditions. We therefore attempted to verify these antibody staining patterns using Flag-tagged recombinant Nek6 and Nek7 proteins. In agreement with localization of endogenous Nek6, Flag-Nek6 was clearly concentrated on microtubules in the mitotic spindle in metaphase, the central spindle in anaphase, and the midbody during cytokinesis (Fig. 7A). In the case of Flag-Nek7, the recombinant protein was also found to associate with the centrosome in some interphase cells but not others, consistent with the Nek7 antibody staining, but no distinct localization could be detected during mitosis. Interestingly, neither of the Flag-tagged proteins could be seen at spindle poles, perhaps due to these sites already being saturated with endogenous protein. In summary, we propose that the bulk of Nek6 and Nek7 is diffusely distributed throughout the cell cycle but that a significant fraction of Nek6 associates with different microtubule-based structures during mitosis and that a small fraction of Nek7 can be found at interphase centrosomes and mitotic spindle poles.

Nek6 and Nek7 interact with and phosphorylate microtubule preparations in vitro. We then examined whether Nek6, or indeed Nek7, was capable of interacting with microtubules using an in vitro sedimentation assay. This revealed that both Nek6 and Nek7 sediment very efficiently with taxol-stabilized microtubules, as does γ-tubulin to a similar extent (Fig. 8A and B). As Nek6 and Nek7 are kinases, we then examined whether they could phosphorylate microtubule preparations in vitro. This revealed that, unlike Nek2, which also binds to microtubules, both Nek6 and Nek7 efficiently phosphorylate proteins that migrate by SDS-PAGE at the size of α- and β-tubulin (Fig. 8C). Thus, Nek6 and Nek7 may directly regulate microtubule organization through phosphorylation of either a microtubule-associated protein (MAP) or, possibly, microtubules themselves.

Nek6 and Nek7 are required for robust mitotic spindle formation and cytokinesis. To investigate the cause of the metaphase arrest seen upon depletion of Nek6 or Nek7 or expression of inactive mutants, we used quantitative immunofluorescence microscopy to examine mitotic spindle structure. While control cells displayed a robust spindle, spindles in cells expressing kinase-inactive Nek6 or Nek7 appeared more fragile, with less-distinct microtubules and less-focused spindle poles (Fig. 9A). There was also a substantial reduction in overall spindle microtubule inten-

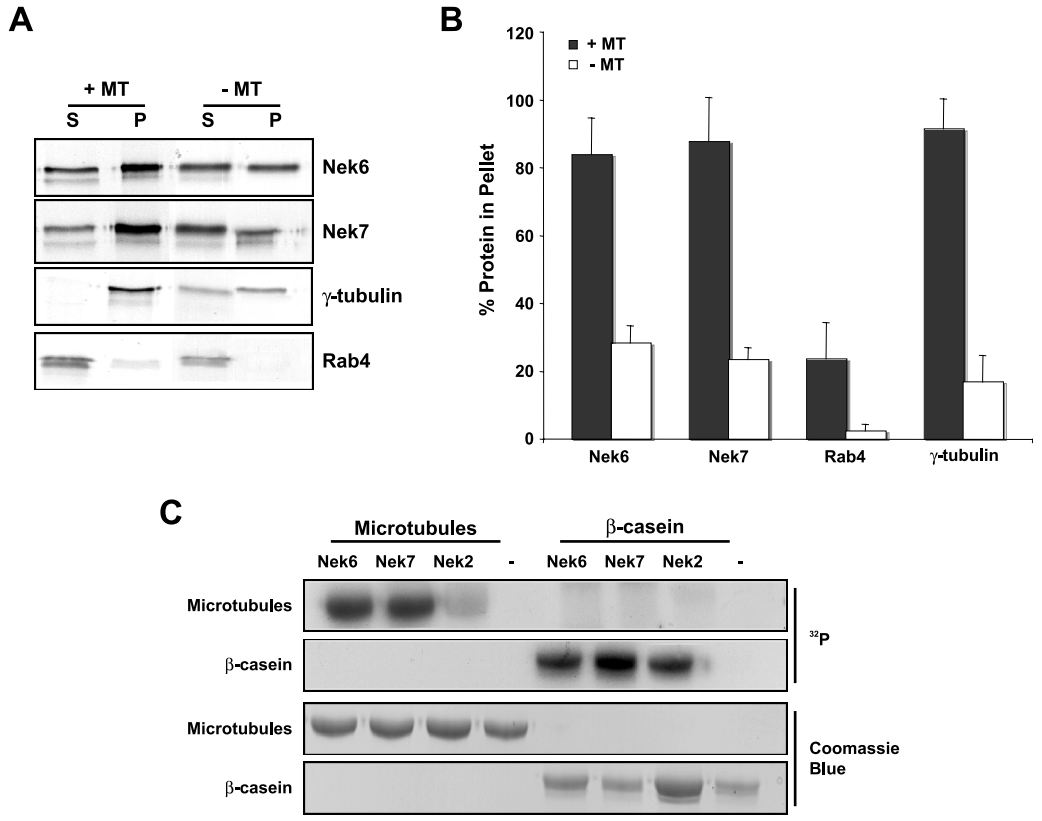

FIG. 8. Nek6 and Nek7 interact with and phosphorylate microtubule preparations in vitro. (A) Nek6 and Nek7 and the control proteins Rab4 and γ-tubulin were generated by in vitro translation in the presence of [^{35}S]methionine. Input proteins were incubated with taxol-stabilized microtubules (+MT) or without taxol-stabilized microtubules (−MT). Proteins were spun at 35,000 rpm on a sucrose cushion for 30 min, and supernatant (S) and pellet (P) fractions were collected and analyzed by SDS-PAGE and autoradiography. (B) The histogram represents the percentages of input protein found within the pellet fractions with and without taxol-stabilized microtubules. Data represent means (±standard deviations) from three separate experiments. (C) Kinase assays were performed for 30 min at 30°C with no kinase (−) or purified recombinant His-tagged Nek6, Nek7, or Nek2 kinases and purified microtubules or β-casein as substrates, before analysis by SDS-PAGE, Coomassie blue staining, and autoradiography (^{32}P).

sity (Fig. 9B). We next determined whether cells expressing kinase-inactive Nek6 or Nek7 proteins had altered spindle stability by determining the rate of spindle collapse in response to 5 μM nocodazole treatment. Cells expressing the completely inactive Nek6-K75M or Nek7-K64M mutants lost spindles more rapidly than cells expressing the wild-type proteins, while the hypomorphic mutants lost spindles at an intermediate rate (Fig. 9C). Cells depleted of Nek6 or Nek7 by RNAi showed similarly fragile spindle structures (Fig. 9D), with considerably reduced α-tubulin intensities and shorter spindle lengths, as determined by pole-to-pole distance measurements (Fig. 9E). This was independent of whether cells were able to undergo apoptosis or not (see Fig. S1 in the supplemental material).

Finally, to directly show that the metaphase arrest was the result of SAC activation, we treated cells depleted of Nek6 or Nek7 with the Aurora B inhibitor ZM 447439 to overcome the SAC. This led to a reduction of more than twofold in cells blocked in metaphase (Fig. 10A). We therefore conclude that Nek6 and Nek7 are required to maintain robust mitotic spindles and that the metaphase arrest is a result of either insufficient attachment of microtubules and/or a lack of tension across the sister chromatids, resulting in activation of the SAC. Importantly, SAC bypass also led to an increase of more than twofold in cells blocked in late mitosis, providing further evidence that these kinases have a second independent role in the completion of cytokinesis (Fig. 10B).

DISCUSSION

Nek6 and Nek7 represent 2 of the 11 NIMA-related kinases encoded by the human genome (27). They are unusual in that their sequences encode little more than a catalytic domain, and they lack the C-terminal regulatory region common to other members of this family. Furthermore, they are closely related to each other, suggesting that they have arisen from a recent gene duplication event and may have redundant functions. Previous data had implicated Nek6 and Nek7 in the regulation of mitosis downstream of another NIMA-related kinase, Nek9, with Nek9 responsible for phosphorylation of key residues within the activation loop of Nek6 and Nek7 (2). However, the published data on Nek6 and Nek7 function were somewhat contradictory, and little was known about the events downstream of these kinases. Here, we have demonstrated that not only are both Nek6 and Nek7 activated in mitotic cells, but interference with Nek6 or Nek7 function, through either RNAi-mediated depletion or expression of catalytically com-

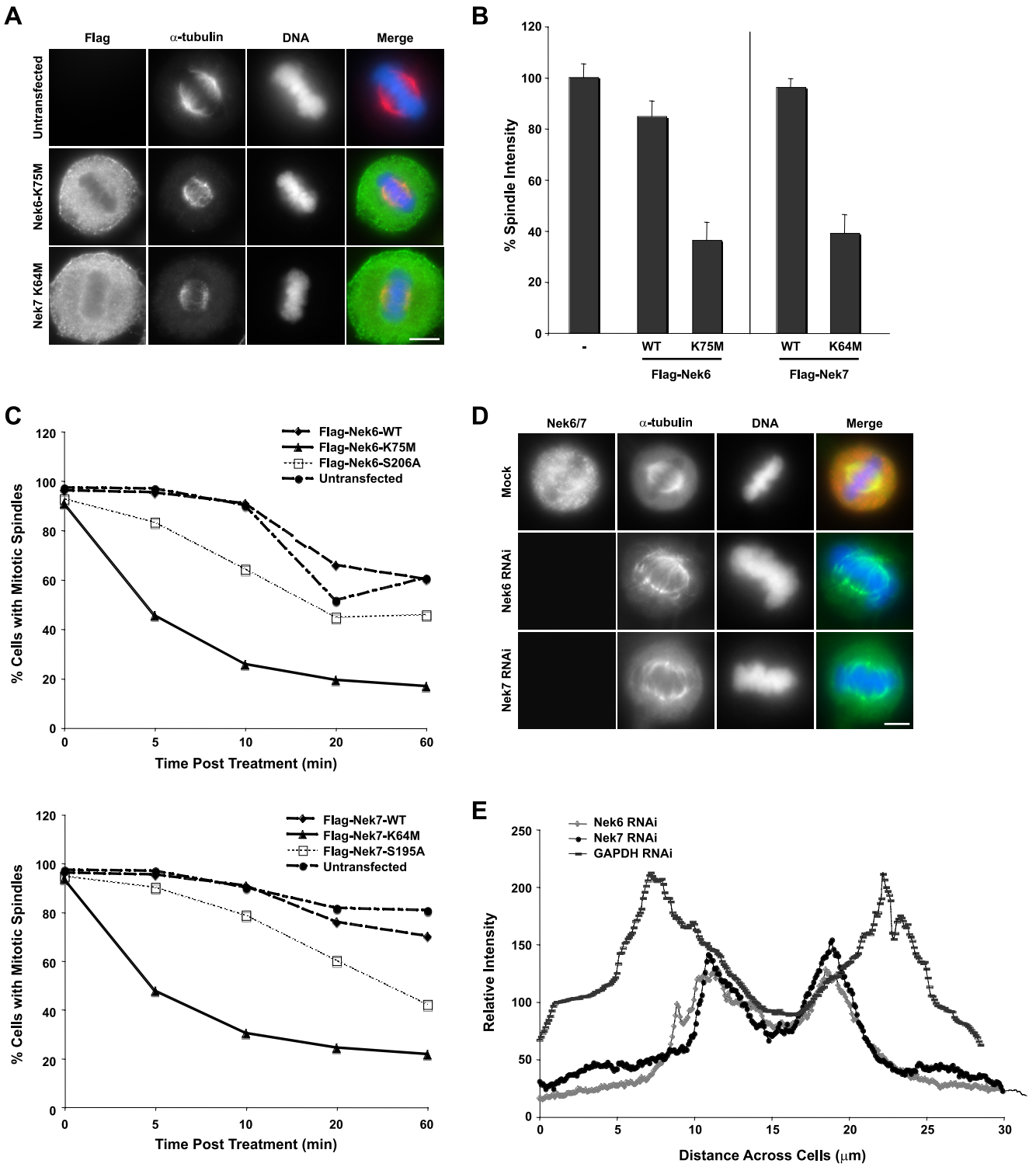

FIG. 9. Nek6 and Nek7 are required for formation of robust mitotic spindles. (A) HeLa cells were either untransfected or transiently transfected with Flag-Nek6-K75M or Flag-Nek7-K64M constructs. After 24 h, cells were processed for immunofluorescence microscopy with Flag antibodies to detect transfected cells (green in merge) and α-tubulin antibodies to detect the microtubule network (red in merge). DNA was stained with Hoechst 33258 (blue). Scale bar, 10 μm. (B) The relative intensity of the metaphase spindle of transfected cells was measured for each construct, using quantitative fluorescence imaging. Data represent means (±standard deviations) from measurements from 50 cells for each construct. The relative spindle intensity is measured as a percentage of the untransfected spindle intensity (−). WT, wild type. (C) HeLa cells were transiently transfected with Flag-Nek6 (top) or Flag-Nek7 (bottom) constructs for 24 h. Cells were then treated with nocodazole before being fixed at the time points indicated. Fixed cells were processed for immunofluorescence microscopy with Flag antibodies to detect transfected cells and α-tubulin antibodies to detect the microtubule network. Transfected mitotic cells were scored for the integrity of their mitotic spindles. Spindles were considered to have collapsed when no clear spindle could be seen within the cell. A total of 30 cells were counted for each construct in three separate experiments. (D) HeLa cells treated with Nek6 or Nek7 siRNA oligonucleotides for 72 h were fixed and analyzed by immunofluorescence microscopy with Nek6 or Nek7 (red in merge) and α-tubulin antibodies (green in merge). DNA was stained with Hoechst 33258 (blue). (E) The relative intensity and length of metaphase spindles in Nek6-, Nek7-, and GAPDH-depleted cells were measured using ImageJ analysis software.

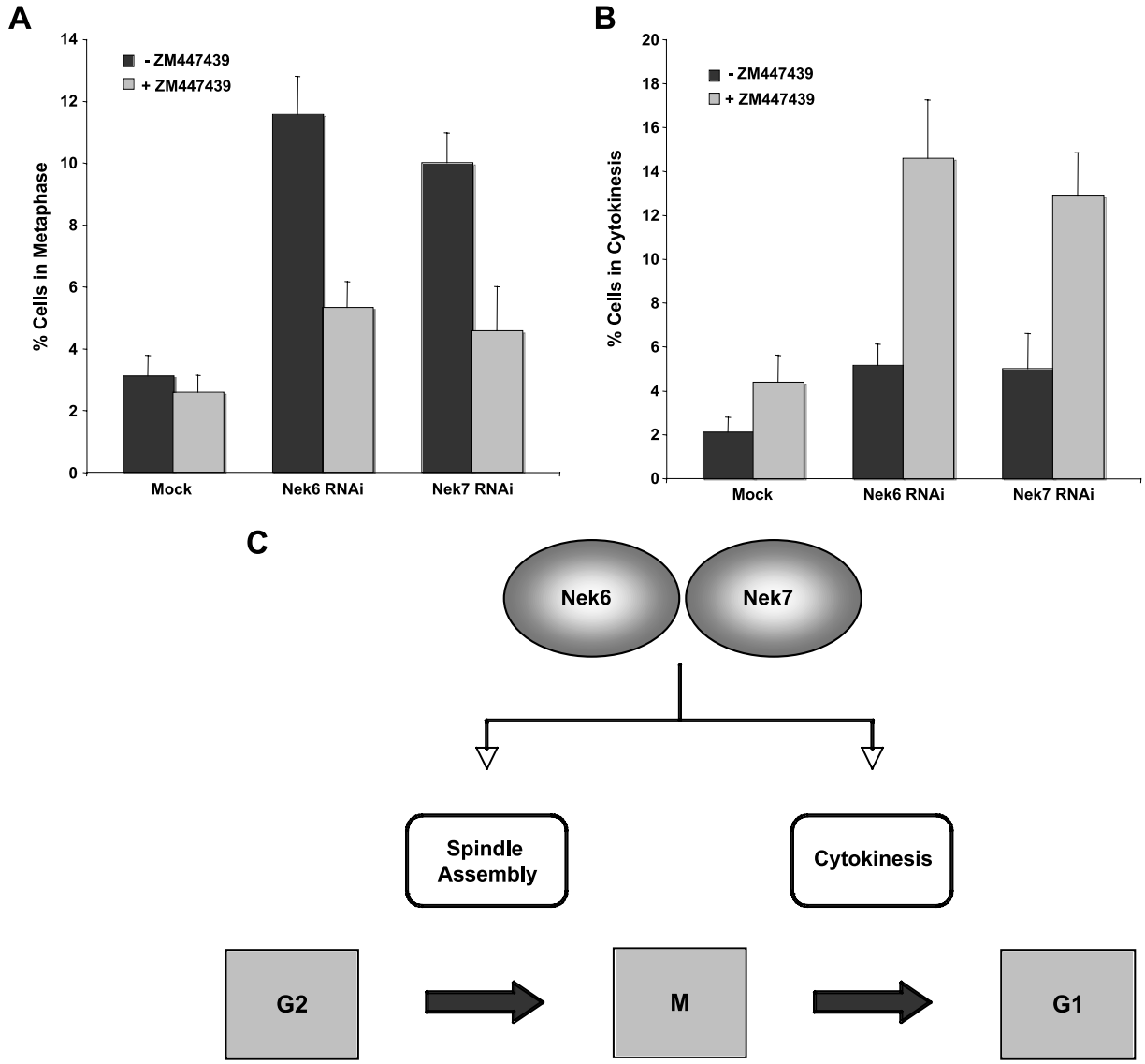

FIG. 10. Overriding the SAC leads to a delay in cytokinesis, in response to Nek6 or Nek7 depletion. (A, B) HeLa cells were mock transfected or transfected with Nek6 or Nek7 siRNA oligonucleotides for 72 h in the presence or absence of the Aurora B inhibitor ZM447439 before being fixed and analyzed by immunofluorescence microscopy. The frequency of cells in metaphase (A) or cytokinesis (B) was scored. Data represent means (±standard deviations) from three separate experiments, with at least 100 cells in each case. (C) Model showing two points of action for the Nek6 and Nek7 kinases in mitotic progression, one in spindle formation and one in cytokinesis. This model is based upon data presented here, showing that depletion of either of the kinases or expression of inactive mutants leads to metaphase arrest, while depletion of either of the kinases in the presence of a SAC inhibitor or expression of hypomorphic mutants leads to a cytokinesis arrest.

promised mutants, leads to mitotic arrest and apoptosis. More importantly, using different conditions of interference, we found two distinct points of action for Nek6 and Nek7 within mitosis, one at metaphase and the other at cytokinesis (Fig. 10C).

Expression of completely inactive Nek6 or Nek7 mutants or depletion of the proteins by RNAi predominantly led to a metaphase arrest, whereas expression of hypomorphic mutants or protein depletion in the presence of an SAC inhibitor led to arrest during cytokinesis. The metaphase arrest was accompanied by the formation of short, nocodazole-sensitive spindles with reduced microtubule density. Gradual loss of chromosome alignment was also detected by time-lapse imaging of cells expressing inactive Nek7. These data are all consistent with reduced nucleation or stability of spindle microtubules, triggering activation of the SAC. Indeed, treatment of depleted cells with an Aurora B inhibitor to bypass the SAC led to a reduction in the frequency of metaphase arrest. Concomitantly, there was an increase in the frequency of cells blocked in cytokinesis under these conditions, while cells expressing the hypomorphic mutants, even in the absence of the SAC inhibitor, also accumulated in cytokinesis. With the hypomorphic Nek7 mutant, time-lapse imaging revealed that cells completed sister chromatid separation and actomyosin ring contraction but failed to undergo abscission. We interpret these data to mean that these kinases have two distinct functions during

mitosis, one at metaphase that requires a certain level of activity and one in late mitosis that requires a higher level of activity. Intriguingly, using phosphospecific antibodies that detect activated Nek6, Rapley et al. (31) showed that Nek6 activity increased 2 h after release from a nocodazole arrest, at the time when they would be progressing through cytokinesis.

One explanation for the fragile spindles is reduced microtubule nucleation at spindle poles. This hypothesis is based on the observations that Nek6, Nek7, and activated Nek9 localize to spindle poles in early mitosis, that Nek9 can interact with the γ-TuRC, and that Nek7 is required to recruit γ-tubulin to spindle poles (19, 32, 40; this study). Indeed, having confirmed that both Nek6 and Nek7 can separately bind to Nek9, we found not surprisingly that both Nek6 and Nek7 are in complexes with γ-tubulin (our unpublished observations). However, we would argue that, at least for Nek6, reduced microtubule nucleation at spindle poles might not be the only cause of spindle defects, as endogenous and recombinant Nek6 predominantly localize to spindle microtubules rather than spindle poles. Moreover, the punctate pattern of Nek6 staining in metaphase and anaphase is highly reminiscent of microtubule plus-end binding proteins, such as EB1 or CLIP-170. In vitro, both Nek6 and Nek7 cosedimented with microtubules and were capable of phosphorylating taxol-stabilized microtubule preparations. Thus, Nek6 may function within the spindle itself to promote either microtubule nucleation or stability through recruitment and/or phosphorylation of tubulins or MAPs. Furthermore, Nek6 may promote interaction of γ-tubulin complexes with preexisting spindle microtubules, supporting the idea that microtubule nucleation within the spindle itself may be as important for spindle organization as nucleation at spindle poles (13).

In further support of this hypothesis, the *Arabidopsis* Nek6 orthologue colocalizes with γ-tubulin complexes on plant cortical microtubules and interacts with the microtubule-dependent armadillo repeat-containing kinesin motor protein ARK1 (24, 34). A kinesin family motor protein, Eg5, has also been reported as a substrate of vertebrate Nek6 (31). Eg5 has diverse microtubule-dependent roles in mitosis, including centrosome separation, organization of microtubules during spindle formation, and antiparallel force generation in the spindle midzone (36). Nek6 phosphorylates Eg5 at Ser-1033, and this may have a role in regulating spindle pole separation (31). Although we did not observe monopolar spindles with unseparated centrosomes upon interference of Nek6 or Nek7, it is entirely plausible that Eg5 phosphorylation by Nek6 does contribute to the correct timing of centrosome separation.

Roles in cytokinesis for NIMA-related kinases were first proposed from studies of lower eukaryotes, with the fission yeast Fin1 regulating components of the septum initiation network and *Drosophila* DmNek2 required for proper organization of anillin and actin at the cleavage furrow (15, 28). Nek6 and Nek7 may similarly regulate the localization of factors required for cytokinesis. Alternatively, they may regulate cytokinesis through stabilizing the microtubules of the central spindle in a similar manner to the way that they act in metaphase. Consistent with this, we found Nek6 to localize not only to microtubules of the metaphase spindle but also to central spindle microtubules in anaphase and the midbody region in cytokinesis. In this regard, it is worth noting that the phosphospecific antibodies raised to the Eg5 Ser-1033 site stained the cleavage furrow, raising the possibility that Nek6 may regulate microtubule-dependent events in late mitosis via Eg5 (31). Although the distinct localization patterns that we observe for Nek6 and Nek7 may reflect different avidities of the antibodies, it supports the idea that these kinases have distinct functions, as indicated by the fact that single depletion of either kinase was sufficient to cause mitotic defects. Interestingly, the only regions of the proteins that exhibit significant sequence divergence are the short N-terminal extensions, and we are currently investigating whether these regions are important not only for their distinct subcellular localization but also for their interactions with potentially different substrate molecules.

Interference with Nek6 or Nek7 function induces a marked growth inhibition, mitotic arrest, and apoptosis (39; this study). This was observed in MDA-MB-468 breast cancer-derived and OVCAR3 ovarian cancer-derived cell lines (data not shown), as well as in HeLa cervical cancer-derived cells. Importantly, apoptosis is dependent upon entry into mitosis, with apoptosis inhibition leading to an increase in the fraction of live cells arrested in mitosis. Thus, small molecule inhibitors of these kinases should kill only cells that are actively dividing. Whether or not these kinases make attractive targets for the development of novel anticancer agents, however, will depend in large part upon whether they are mutated or exhibit altered expression in human cancers, as immortalized but nontransformed RPE1-hTERT cells also underwent apoptosis in response to Nek6 interference. While data on this point remain rather limited, there are reports that expression of these kinases is upregulated in a number of common cancers, including breast, colorectal, lung, and larynx as well as liver and gastric tumors and non-Hodgkin's lymphoma (3, 4, 35). Furthermore, Nek6 and Nek7 mutations have been detected during genomewide screenings of human cancers, although the effect that these have on kinase activity has yet to be determined (5, 16). In summary, our studies have revealed that Nek6 and Nek7 contribute to at least two distinct events during mitotic progression. The future development of analogue-sensitive kinases that can be inactivated rapidly and selectively will be of great benefit for dissecting these events.

ACKNOWLEDGMENTS

We are very grateful to Jon Pines (Cambridge, United Kingdom), Dina Dikovskaya and Axel Knebel (Dundee, United Kingdom), Richard Bayliss (London, United Kingdom), and Kayoko Tanaka (Leicester, United Kingdom) for helpful comments on this work and all members of our laboratory for useful discussion. We also thank Roger Snowden (Leicester, United Kingdom) for support with flow cytometry.

This work was funded by grants to A.M.F. from the Wellcome Trust, Millennium Pharmaceuticals, and AstraZeneca.

REFERENCES

1. **Bahe, S., Y. D. Stierhof, C. J. Wilkinson, F. Leiss, and E. A. Nigg.** 2005. Rootletin forms centriole-associated filaments and functions in centrosome cohesion. J. Cell Biol. **171:**27–33.
2. **Belham, C., J. Roig, J. A. Caldwell, Y. Aoyama, B. E. Kemp, M. J. Comb, and J. Avruch.** 2003. A mitotic cascade of NIMA family kinases. J. Biol. Chem. **278:**34897–34909.
3. **Capra, M., P. G. Nuciforo, S. Confalonieri, M. Quarto, M. Bianchi, M. Nebuloni, R. Boldorini, F. Pallotti, G. Viale, M. L. Gishizky, G. F. Draetta,**

and P. P. Di Fiore. 2006. Frequent alterations in the expression of serine/threonine kinases in human cancers. Cancer Res. **66:**8147–8154.

4. **Chen, J., L. Li, Y. Zhang, H. Yang, Y. Wei, L. Zhang, X. Liu, and L. Yu.** 2006. Interaction of Pin1 with Nek6 and characterization of their expression correlation in Chinese hepatocellular carcinoma patients. Biochem. Biophys. Res. Commun. **341:**1059–1065.
5. **Davies, H., C. Hunter, R. Smith, P. Stephens, C. Greenman, G. Bignell, J. Teague, A. Butler, S. Edkins, C. Stevens, A. Parker, S. O'Meara, T. Avis, S. Barthorpe, L. Brackenbury, G. Buck, J. Clements, J. Cole, E. Dicks, K. Edwards, S. Forbes, M. Gorton, K. Gray, K. Halliday, R. Harrison, K. Hills, J. Hinton, D. Jones, V. Kosmidou, R. Laman, R. Lugg, A. Menzies, J. Perry, R. Petty, K. Raine, R. Shepherd, A. Small, H. Solomon, Y. Stephens, C. Tofts, J. Varian, A. Webb, S. West, S. Widaa, A. Yates, F. Brasseur, C. S. Cooper, A. M. Flanagan, A. Green, M. Knowles, S. Y. Leung, L. H. Looijenga, B. Malkowicz, M. A. Pierotti, B. T. Teh, S. T. Yuen, S. R. Lakhani, D. F. Easton, B. L. Weber, P. Goldstraw, A. G. Nicholson, R. Wooster, M. R. Stratton, and P. A. Futreal.** 2005. Somatic mutations of the protein kinase gene family in human lung cancer. Cancer Res.**65:**7591–7595.
6. **De Souza, C. P., K. P. Horn, K. Masker, and S. A. Osmani.** 2003. The SONB(NUP98) nucleoporin interacts with the NIMA kinase in Aspergillus nidulans. Genetics **165:**1071–1081.
7. **De Souza, C. P. C., A. H. Osmani, L.-P. Wu, J. L. Spotts, and S. A. Osmani.** 2000. Mitotic histone H3 phosphorylation by the NIMA kinase in *Aspergillus nidulans*. Cell **102:**293–302.
8. **Feige, E., and B. Motro.** 2002. The related murine kinases, Nek6 and Nek7, display distinct patterns of expression. Mech. Dev. **110:**219–223.
9. Reference deleted.
10. **Fry, A. M., P. Meraldi, and E. A. Nigg.** 1998. A centrosomal function for the human Nek2 protein kinase, a member of the NIMA-family of cell cycle regulators. EMBO J. **17:**470–481.
11. **Fry, A. M., and E. A. Nigg.** 1997. Characterization of mammalian NIMA-related kinases. Methods Enzymol. **283:**270–282.
12. **Gadde, S., and R. Heald.** 2004. Mechanisms and molecules of the mitotic spindle. Curr. Biol. **14:**R797–R805.
13. **Goshima, G., R. Wollman, S. S. Goodwin, N. Zhang, J. M. Scholey, R. D. Vale, and N. Stuurman.** 2007. Genes required for mitotic spindle assembly in Drosophila S2 cells. Science **316:**417–421.
14. **Grallert, A., and I. M. Hagan.** 2002. *S. pombe* NIMA related kinase, Fin1, regulates spindle formation, and an affinity of Polo for the SPB. EMBO J. **21:**3096–3107.
15. **Grallert, A., A. Krapp, S. Bagley, V. Simanis, and I. M. Hagan.** 2004. Recruitment of NIMA kinase shows that maturation of the S. pombe spindle-pole body occurs over consecutive cell cycles and reveals a role for NIMA in modulating SIN activity. Genes Dev. **18:**1007–1021.
16. **Greenman, C., P. Stephens, R. Smith, G. L. Dalgliesh, C. Hunter, G. Bignell, H. Davies, J. Teague, A. Butler, C. Stevens, S. Edkins, S. O'Meara, I. Vastrik, E. E. Schmidt, T. Avis, S. Barthorpe, G. Bhamra, G. Buck, B. Choudhury, J. Clements, J. Cole, E. Dicks, S. Forbes, K. Gray, K. Halliday, R. Harrison, K. Hills, J. Hinton, A. Jenkinson, D. Jones, A. Menzies, T. Mironenko, J. Perry, K. Raine, D. Richardson, R. Shepherd, A. Small, C. Tofts, J. Varian, T. Webb, S. West, S. Widaa, A. Yates, D. P. Cahill, D. N. Louis, P. Goldstraw, A. G. Nicholson, F. Brasseur, L. Looijenga, B. L. Weber, Y. E. Chiew, A. DeFazio, M. F. Greaves, A. R. Green, P. Campbell, E. Birney, D. F. Easton, G. Chenevix-Trench, M. H. Tan, S. K. Khoo, B. T. Teh, S. T. Yuen, S. Y. Leung, R. Wooster, P. A. Futreal, and M. R. Stratton.** 2007. Patterns of somatic mutation in human cancer genomes. Nature **446:**153–158.
17. **Hames, R. S., R. E. Crookes, K. R. Straatman, A. Merdes, M. J. Hayes, A. J. Faragher, and A. M. Fry.** 2005. PCM-1 dynamic recruitment of Nek2 kinase to the centrosome involves microtubules, and localized proteasomal degradation. Mol. Biol. Cell **16:**1711–1724.
18. **Holland, P. M., A. Milne, K. Garka, R. S. Johnson, C. Willis, J. E. Sims, C. T. Rauch, T. A. Bird, and G. D. Virca.** 2002. Purification, cloning and characterization of Nek8, a novel NIMA-related kinase, and its candidate substrate Bicd2. J. Biol. Chem. **277:**16229–16240.
19. **Kim, S., K. Lee, and K. Rhee.** 2007. NEK7 is a centrosomal kinase critical for microtubule nucleation. Biochem. Biophys. Res. Commun. **360:**56–62.
20. **Krien, M. J., R. R. West, U. P. John, K. Koniaras, J. R. McIntosh, and M. J. O'Connell.** 2002. The fission yeast NIMA kinase Fin1p is required for spindle function and nuclear envelope integrity. EMBO J. **21:**1713–1722.
21. **Mayor, T., U. Hacker, Y. D. Stierhof, and E. A. Nigg.** 2002. The mechanism regulating the dissociation of the centrosomal protein C-Nap1 from mitotic spindle poles. J. Cell Sci. **115:**3275–3284.
22. **Mayor, T., Y. D. Stierhof, K. Tanaka, A. M. Fry, and E. A. Nigg.** 2000. The centrosomal protein C-Nap1 is required for cell cycle-regulated centrosome cohesion. J. Cell Biol. **151:**837–846.
23. **Minoguchi, S., M. Minoguchi, and A. Yoshimura.** 2003. Differential control of the NIMA-related kinases, Nek6 and Nek7, by serum stimulation. Biochem. Biophys. Res. Commun. **301:**899–906.
24. **Motose, H., R. Tominaga, T. Wada, M. Sugiyama, and Y. Watanabe.** 2008. A NIMA-related protein kinase suppresses ectopic outgrowth of epidermal cells through its kinase activity and the association with microtubules. Plant J. **54:**829–844.
25. **Nigg, E. A.** 2001. Mitotic kinases as regulators of cell division and its checkpoints. Nat. Rev. Mol. Cell Biol. **2:**21–32.
26. **O'Connell, M. J., M. J. Krien, and T. Hunter.** 2003. Never say never. The NIMA-related protein kinases in mitotic control. Trends Cell Biol. **13:**221–228.
27. **O'Regan, L., J. Blot, and A. M. Fry.** 2007. Mitotic regulation by NIMA-related kinases. Cell Div. **2:**25.
28. **Prigent, C., D. M. Glover, and R. Giet.** 2005. Drosophila Nek2 protein kinase knockdown leads to centrosome maturation defects while overexpression causes centrosome fragmentation and cytokinesis failure. Exp. Cell Res. **303:**1–13.
29. **Quarmby, L. M., and M. R. Mahjoub.** 2005. Caught Nek-ing: cilia and centrioles. J. Cell Sci. **118:**5161–5169.
30. **Rapley, J., J. E. Baxter, J. Blot, S. L. Wattam, M. Casenghi, P. Meraldi, E. A. Nigg, and A. M. Fry.** 2005. Coordinate regulation of the mother centriole component Nlp by Nek2 and Plk1 protein kinases. Mol. Cell. Biol. **25:**1309–1324.
31. **Rapley, J., M. Nicolas, A. Groen, L. Regue, M. T. Bertran, C. Caelles, J. Avruch, and J. Roig.** 2008. The NIMA-family kinase Nek6 phosphorylates the kinesin Eg5 at a novel site necessary for mitotic spindle formation. J. Cell Sci. **121:**3912–3921.
32. **Roig, J., A. Groen, J. Caldwell, and J. Avruch.** 2005. Active Nercc1 protein kinase concentrates at centrosomes early in mitosis and is necessary for proper spindle assembly. Mol. Biol. Cell **16:**4827–4840.
33. **Roig, J., A. Mikhailov, C. Belham, and J. Avruch.** 2002. Nercc1, a mammalian NIMA-family kinase, binds the Ran GTPase and regulates mitotic progression. Genes Dev. **16:**1640–1658.
34. **Sakai, T., H. Honing, M. Nishioka, Y. Uehara, M. Takahashi, N. Fujisawa, K. Saji, M. Seki, K. Shinozaki, M. A. Jones, N. Smirnoff, K. Okada, and G. O. Wasteneys.** 2008. Armadillo repeat-containing kinesins and a NIMA-related kinase are required for epidermal-cell morphogenesis in Arabidopsis. Plant J. **53:**157–171.
35. **Takeno, A., I. Takemasa, Y. Doki, M. Yamasaki, H. Miyata, S. Takiguchi, Y. Fujiwara, K. Matsubara, and M. Monden.** 2008. Integrative approach for differentially overexpressed genes in gastric cancer by combining large-scale gene expression profiling and network analysis. Br. J. Cancer **99:**1307–1315.
36. **Walczak, C. E., and R. Heald.** 2008. Mechanisms of mitotic spindle assembly and function. Int. Rev. Cytol. **265:**111–158.
37. **Wiese, C., and Y. Zheng.** 2006. Microtubule nucleation: gamma-tubulin and beyond. J. Cell Sci. **119:**4143–4153.
38. **Wu, L., S. A. Osmani, and P. M. Mirabito.** 1998. A role for NIMA in the nuclear localization of cyclin B in *Aspergillus nidulans*. J. Cell Biol. **141:**1575–1587.
39. **Yin, M.-J., L. Shao, D. Voehringer, T. Smeal, and B. Jallal.** 2003. The serine/threonine kinase Nek6 is required for cell cycle progression through mitosis. J. Biol. Chem. **278:**52454–52460.
40. **Yissachar, N., H. Salem, T. Tennenbaum, and B. Motro.** 2006. Nek7 kinase is enriched at the centrosome, and is required for proper spindle assembly and mitotic progression. FEBS Lett. **580:**6489–6495.